FURTHER INTERPRETATION OF THE Cu–Fe–Ni SULFIDE MINERALIZATION IN THE DULUTH COMPLEX, NORTHEASTERN MINNESOTA

JILL DILL PASTERIS

Department of Earth and Planetary Sciences, McDonnell Center for the Space Sciences, Washington University, Box 1169, St. Louis, Missouri 63130, U.S.A.

ABSTRACT

Approximately 20 samples mineralized with Cu, Fe and Ni sulfides from the South Kawishiwi (Inco deposit) and Partridge River (Minnamax deposit) intrusive complexes were studied by means of the optical microscope and the electron microprobe. Cathodoluminescence, microthermometry and laser-Raman spectroscopy were used on some samples. In the two suites, both dominated by troctolite, the sulfides are mineralogically similar (predominantly pyrrhotite, pentlandite, chalcopyrite, cubanite) and also texturally similar. In the Inco suite, however, both magnetite and ilmenite are present, whereas troilite is rare. In contrast, the occurrence of troilite and vapor-deposited graphite, as also the presence of ilmenite without magnetite, in the suite from Minnamax, suggests that the environment there was more reducing than at Inco. The following observations show that a mobile, reactive fluid phase was active during late-stage magmatism: vapor-deposited graphite in fractures in unaltered silicates, Cl-bearing secondary fluid-inclusions in olivine, replacement of coarse pyrrhotite segregations by massive cubanite, and precipitates of fine-grained iron–nickel sulfide along fractures in serpentinized olivine. Widely variable compositions of pentlandite also suggest partial postmagmatic re-equilibration. Both an early immiscible sulfide melt (with a high Fe:Cu ratio) and a later Cu-enriched magmatic fluid produced mineralization in the troctolites, the sulfide melt by primary precipitation, the Cu-bearing fluid mainly by replacement. The movement and composition of the fluid were controlled by normal intercumulus processes in the complex. This hypothesis is in accord with the sulfur-isotope data of Ripley (1981) for the Dunka Road deposit in the Partridge River pluton.

Keywords: Cu, Fe and Ni sulfides, Duluth complex, Partridge River pluton, Minnamax deposit, South Kawishiwi pluton, Inco deposit, Minnesota.

SOMMAIRE

On a étudié au microscope et à la microsonde environ 20 échantillons minéralisés en sulfures de Cu, Fe et Ni des complexes intrusifs de South Kawishiwi (gîte Inco) et Partridge River (gîte Minnamax). Certains échantillons furent étudiés par cathodoluminescence, microthermométrie et spectroscopie Raman au laser. Dans les deux suites, dominées par la troctolite, les sulfures (surtout: pyrrhotine, pentlandite, chalcopyrite, cubanite) sont minéralogiquement et texturellement semblables. Dans la suite Inco, la magnétite et l'ilménite sont présentes, alors que la troïlite y est rare. Par contre, la présence de troïlite et de graphite, déposé en phase vapeur, et d'ilménite sans magnétite, dans la suite Minnamax, indiqueraient un milieu plus réducteur que celui du gîte Inco. Les observations suivantes montrent qu'une phase fluide mobile réactive fut active au stade tardif du magmatisme: graphite déposé par phase vapeur dans les fractures de silicates non altérés, inclusions fluides secondaires chlorifères dans l'olivine, remplacement d'agrégats grossiers de pyrrhotine par de la cubanite massive, et précipités de sulfure de fer et nickel à grain fin le long de fractures dans l'olivine serpentinisée. La grande variation de composition de la pentlandite indiquerait aussi un rééquilibre post-magmatique partiel. Un bain sulfuré immiscible précoce (à rapport Fe:Cu élevé) et un fluide magmatique ultérieur enrichi en cuivre sont responsables de la minéralisation dans les troctolites: le liquide sulfuré, par précipitation primaire et le fluide cuprifère, surtout par remplacement. Le mouvement et la composition du fluide durent avoir été gouvernés par un processus intercumulus normal dans le complexe intrusif, hypothèse qui du moins concorde avec les données sur isotopes du soufre (Ripley 1981) pour le gîte de Dunka Road, situé dans le pluton de Partridge River.

Traduit par la Rédaction)

Mots-clés: sulfures de Cu, Fe et Ni, complexe de Duluth, pluton de Partridge River, gîte Minnamax, pluton de South Kawishiwi, gîte Inco, Minnesota.

INTRODUCTION

Sample location

Approximately 20 specimens of mineralized drill-core and hand samples were studied from the Inco and Minnamax mines sites in the Duluth Complex (Fig. 1). The Inco material (provided by M. Boucher) consists predominantly of troctolites and augite-bearing troctolites from the South Kawishiwi intrusive body, near the site of the Inco shaft (Cooper *et al.* 1978; Fig. 1 of this paper). The exact localities of the individual samples are not documented.

The Minnamax samples, representing a section of the adjacent Partridge River troctolite body, are macroscopically similar to the Inco suite. These documented drill-core samples are from hole 146 in the southern end of the Tiger Boy deposit, and repre-
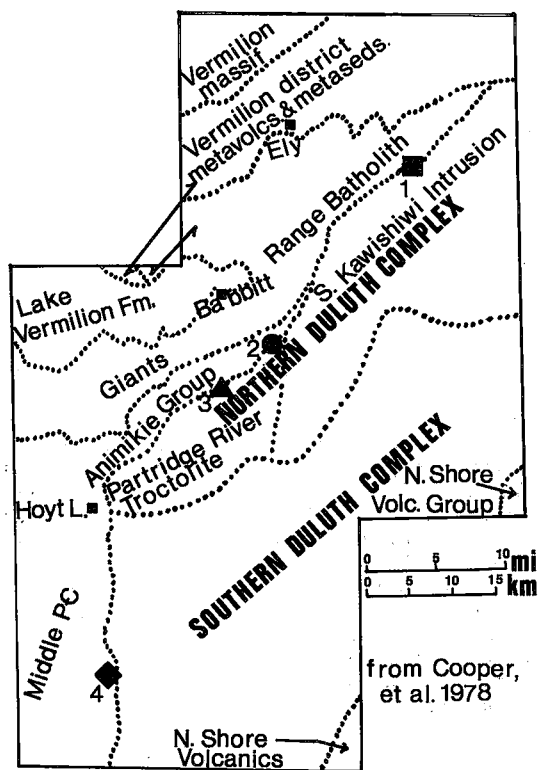
FIG. 1. Generalized geologic map of a portion of the Duluth Complex, showing sampling areas and other sulfide deposits. 1 Inco site, 2 Minnamax site, 3 U.S. Steel site, 4 Water Hen intrusive complex (map after Cooper *et al.* 1978 and Ripley 1981).

sent depth levels of 173 to 586 metres (samples provided by S. Watowich, AMAX). The mine site is presently owned by Kennecott, but the name Minnamax is retained here because AMAX was the operator during this program of drilling and sampling. The silicate rock-types are predominantly troctolitic, but a hornfels zone that may represent xenoliths of underlying metasedimentary and metavolcanic rocks also was sampled. The Cu-Ni sulfide mineralization consists of both the disseminated and massive (Local Boy) type (Watowich 1978).

Techniques of analysis

This overview involved a study by optical microscopy of about 20 doubly polished thin sections in transmitted and reflected light. Microthermometry, Raman spectroscopy and cathodoluminescence were performed on several samples. The initial Raman-microprobe analysis of fluid inclusions and fine-grained graphite was done by F. Adar (Instruments SA) and F. Purcell (Spex Corp.). The author performed later analyses with an Instruments SA Ramanor U-1000. Quantitative wavelength-dispersion analysis (WDS) was carried out on selected sulfides, oxides and silicates with a fully automated JEOL 733 electron microprobe at Washington University. The standards are natural minerals and synthetic materials. Correction procedures for the analyses are based on Bence & Albee (1968) and Albee & Ray (1970). The operating conditions were 15 kV accelerating voltage with currents of 50 nA for oxide, 30 nA for feldspar and 30 nA for sulfide phases. The sulfide data are the primary concern of this paper.

Previous studies

Two previous detailed studies addressed the mineralogy, textures, relative abundances and compositions of sulfide phases in troctolitic sequences at the Inco site and in a drill hole south of Babbitt [Weiblen & Morey (1976) and Boucher (1975), respectively]. Other reports describe the more general geological relationships of the sulfide deposits to the Duluth Complex as well as their economic potential (*e.g.,* Bonnichsen 1972, 1974, Tyson & Chang 1984).

More recently, oxygen- and sulfur-isotope analyses have been performed on the Dunka Road deposit (Ripley & Rao 1980, Ripley 1981) and rubidium and strontium-isotope analyses on a Minnamax drill core (Grant & Molling 1981), both in the Partridge River troctolite. The above studies, together with the sulfur-isotope work of Mainwaring & Naldrett (1977) on the Cu-Ni mineralization in the Water Hen intrusive complex to the south, suggest that reaction of melt and country rocks may have strongly affected the sulfide precipitation in the Duluth Complex; they concluded that much of the sulfur may have been derived from the intruded sediments. The chemistry and physical transport aspects of the mechanism remain to be explained. It thus appears, from petrographic and strontium-isotope analysis (Grant & Molling 1981), that vast amounts of the underlying carbonaceous, sulfide-bearing Virginia Formation were not physically assimilated by the Duluth magmas. However, H_2O, CO_2 and other volatiles may have been selectively assimilated by the melt (*cf.* Weiblen & Morey 1976, Hollister 1980, Ripley 1981).

The immediate aims of the present study are (1) to compare and contrast sulfide relationships observed in the two deposits chosen (Table 1) with previously reported and (2) to re-interpret these data in light of more recent information on the composition of late magmatic fluids and on intercumulus processes. Of particular concern are the following points: the timing of sulfide immiscibility in the magmatic sequence, the factors causing sulfide

TABLE 1. MINERALOGY OF TWO OCCURRENCES OF SULFIDES IN THE DULUTH COMPLEX

Sample	Po	Tr	Cp	Cb	Coarse graphite	Graphite in veinlets	Coarse ilmenite	Coarse magnetite	Fine spinel & ilm. lamellae in silicates
INCO	A	R	A	A	S	N	A	A	A in plag & Cpx
MINNAMAX	A	S	A	A	S	S	A	N	A in plag & Cpx

Key to abbreviations: A abundant, S some, R rare, N not observed, Po pyrrhotite, Tr troilite, Cp chalcopyrite, Cb cubanite.

precipitation, the number of episodes of mineralization and the possibility of subsequent remobilization of sulfides. As documented by previous investigators (*e.g.*, Foose 1982, Tyson & Chang 1984), the individual troctolite bodies at Duluth represent multiple injections of melt and locally strong interaction with wallrock. With the small number of samples in the present study, only broad-scale differences between the suites can be recognized.

The following abbreviations are used in the text and figure captions: Cp chalcopyrite, Cb cubanite, Pn pentlandite, Bn bornite, Tr troilite, Po pyrrhotite, mPo monoclinic pyrrhotite, hPo hexagonal pyrrhotite, ss solid solution, WDS wavelength-dispersion spectroscopy, and EDS energy-dispersion spectroscopy on the electron microprobe. In the sample numbers for the Minnamax drill-core specimens. *i.e.*, 146–XXXX, the second part of the number refers to the depth (in feet).

OPAQUE MINERAL-SILICATE RELATIONSHIPS

Textural relationships of the sulfides are very

similar in the Inco and Minnamax troctolitic samples; the samples, therefore, will be considered together.

Sulfide mineralogy and textural types

Samples from the Minnamax Tiger Boy deposit represent massive mineralization of the Local Boy type (~ 586 m depth), disseminated sulfides in the basal zone (~ 490 m depth), and the "cloud zone" mineralization (~ 335 m depth) that typically lies 200 or more metres above the basal sulfide zone (Watowich 1978). Values of the Cu–Ni ratio reported in AMAX assays range from 2.25 in an isolated zone of hornfels to 5.01 in the upper basal zone. The values are quite erratic, but average about 4.2, which is distinctly higher than the average Cu–Ni ratio in the Inco deposits to the north (Spruce Road ~ 2.7, Maturi ~ 3.3) and of the U.S. Steel deposit (~ 3.3) immediately to the south (S. Watowich, pers. comm. 1982).

The dominant sulfide minerals in the Inco and Minnamax samples are pyrrhotite (in some cases, two compositions), chalcopyrite, cubanite and pentland-

TABLE 2. REPRESENTATIVE BULK COMPOSITION OF SULFIDES

Sample*	Troilite(3)	Pyrrhotite (7)	Chalcopy- rite(5)	Cubanite(7)	Bornite(3)	Ni-Mackina- wite(6)	Heazlewood- ite(2)	Cp?(3)	Bn?(3)
				Compositions in weight percent					
Fe	63.83(.23)	60.64(.19)	30.47(.29)	41.49(.37)	11.75(.24)	58.66(.74)	2.07(.01)	29.27(.24)	13.65(.57)
Ni	0.0 (0)	0.21(.10)	0.02(.02)	0.0 (0)	0.05(.04)	4.97(.16)	69.51(1.15)	0.16(.28)	0.13(.19)
Cu	0.06(.10)	0.20(.20)	34.31(.58)	22.88(.37)	62.20(.45)	0.44(.06)	1.34(.13)	36.01(.33)	57.95(1.79)
Co	0.0 (0)	0.01(.01)	0.0 (.01)	0.0 (0)	0.02(.02)	0.02(.38)	0.01(.01)	0.03(.02)	0.03(.04)
S	36.57(.13)	38.41(.51)	34.51(.47)	35.24(.44)	26.44(.57)	35.12(.81)	28.54(1.63)	34.30(.40)	27.31(1.01)
Total	100.46(.42)	99.47(.40)	99.31(.55)	99.61(.42)	100.46(.68)	99.21(.86)	101.47(.36)	99.77(.80)	99.07(.55)
				Compositions in atomic percent					
Fe	50	48	25	34	10	46.8	2	24	12
Ni	--	--	--	--	--	3.9	56	--	--
Cu	--	--	25	16	49	.01	1	26	45
Co	--	--	--	--	--	--	--	--	--
S	50	52	50	50	41	48.8	41	50	43
Formula	MS	M_9S_{10}	M_2S_2	M_3S_3	$M_{5.76}S_4$	$M_{1.05}S$	$M_{2.88}S_2$	$M_{1.98}S_2$	$M_{5.31}S_4$
	FeS	Fe_9S_{10}	$CuFeS_2$	$Cu_{.96}Fe_{2.04}S_3$	$Cu_{4.78}Fe_{.98}S_4$	$Fe_{.96}Ni_{.08}S$	$Ni_{2.73}Fe_{.10}Cu_{.05}S_2$	$Cu_{1.02}Fe_{.96}S_2$	$Cu_{4.19}Fe_{1.12}S_4$

*Parentheses after sample name indicate number of analyses that were averaged. Parentheses after wt.% analyses show one standard deviation.

Troilite: 146-1961 (AMAX), darker region of Po-Tr intergrowth. Pyrrhotite: DG4 (INCO), grains include large intercumulus Po, Po-Pn, Po-Cp. Chalcopyrite: DG3 (INCO), grains include coarse Cp lamellae in Cb, stringer in silicate, Cp-Po. Cubanite: 146-1691 (AMAX), grains include Cb lamellae in Cp, Cb-Po, Cb-Cp-Po, stringer in silicate. Bornite: 146-1176 & 156-569. Ni-mackinawite: DG3 (INCO), grains include altered bleb, stringer in silicate. Heazlewoodite: 146-569 (AMAX), small grain in Cp-Bn-Hz. Cp?: 146-569 (AMAX), grains include "Cp"-Bn-Pn, bluish and tarnished isolated grains. Bn?: 146-1176, Cp-"Bn" and Cp-"Bn"-Pn; compositions similar to those in 146-569. Electron-microprobe data.

ite, all in widely varying proportions. Quantitative electron-microprobe analysis (Table 2) confirmed the presence of cubanite and chalcopyrite, but not of the related lower-temperature Cu–Fe sulfides talnakhite, mooihoekite and haycockite. Lesser amounts of mackinawite, bornite and an unknown Cu-rich Cu–Fe-sulfide also were identified optically and by electron-microprobe analysis.

Weiblen's & Morey's (1976) sulfide–silicate textural classification is applicable to both the Inco and AMAX samples: 1) interstitial sulfides, bearing an intercumulus relationship to the plagioclase network, 2) sulfide inclusions in plagioclase and clinopyroxene, 3) fine sulfide veinlets traversing grains of serpentinized olivine as well as of unaltered silicates, and 4) sulfide–silicate and sulfide–oxide intergrowths.

Interstitial sulfides are the dominant textural type in both the Inco and AMAX samples (Fig. 2). They consist of massive polygonal blebs of pyrrhotite, pentlandite, chalcopyrite ± cubanite, which are locally accompanied by a halo of irregular, finely dispersed sulfides. The textures are intercumulate.

Considered in the category of included sulfides are abundant, dominantly Cu-rich, elongate sulfide bodies parallel to the (010) planes (*i.e.*, albite twin-lamellae) in the intercumulus plagioclase grains and in adcumulus plagioclase overgrowths. Olivine grains, in contrast, rarely have sulfide inclusions (as noted also by Weiblen & Morey 1976).

Several types of narrow veinlets of opaque phases are present in the Inco and AMAX silicates. The widest veinlets (10–20 μm on average) cross-cut silicate grains and appear to connect the large (up to a few millimetres) bodies of interstitial sulfide. The wider veinlets contain optically identifiable pyrrhotite, pentlandite, chalcopyrite and cubanite (confirmed by electron microprobe). Weiblen & Morey (1976) believed that some veinlets consist solely of chalcopyrite and cubanite. Owing to the small grain-size of the sulfide veinlets, point counting was not possible. However, it appears that veinlets connecting larger sulfide bodies have the same mineralogy as the bodies, whereas isolated narrow veinlets within silicate grains may be Cu-enriched.

Two other types of veinlets are restricted to serpentinized olivine grains: secondary sulfide and oxide stringers. These, commonly, are only a few micrometres in width, but locally are very abundant (Fig. 3). The sulfide veinlets consist of a mottled white, polygranular, strongly anisotropic Ni–mackinawite (Table 2). Other thin veinlets consist of magnetite (optical and microprobe confirmation), which is physically separate from the sulfide stringers, although both opaque phases commonly occur in the same silicate grain.

There is a wide variety of intergrowths (sulfide-silicate, sulfide–oxide, sulfide–sulfide), whose proper interpretation may help to define more precisely the timing and mechanisms of sulfide movement in the troctolites. It should be kept in mind, however, that small-scale textural anomalies and re-equilibration can lead to confusion. Although sulfides commonly lie directly adjacent to or within grains of a mafic silicate (clinopyroxene, biotite, more rarely hornblende) and oxide (magnetite, ilmenite), much of the sulfide is in contact with plagioclase only (*cf.* Ripley 1981, Dunka Road deposit).

As emphasized by Boucher (1975), there are abundant cases of replacement textures among the
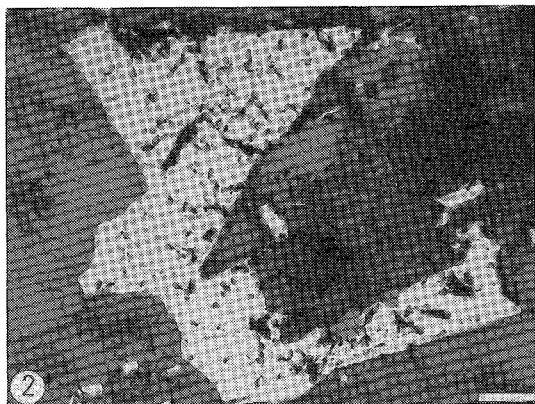

FIG. 2. Interstitial grain of sulfide between plagioclase grains. Sulfide is predominantly massive cubanite with small grains of chalcopyrite (not distinguishable in photograph) around the edge. Reflected light. Scale bar 200 μm. Minnamax drill-core 146, 500 m depth.
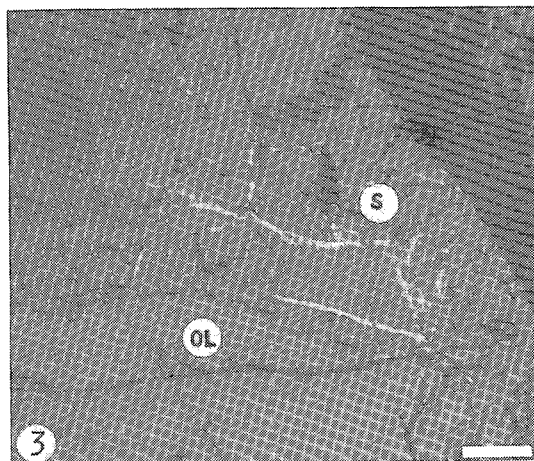

FIG. 3. Iron sulfide veinlets in serpentinized olivine. The sulfide is strongly anisotropic, and in some cases is Ni-mackinawite. OL olivine, S serpentine. Reflected light, dry objective. Scale bar 1 mm. Inco sample DG–8.
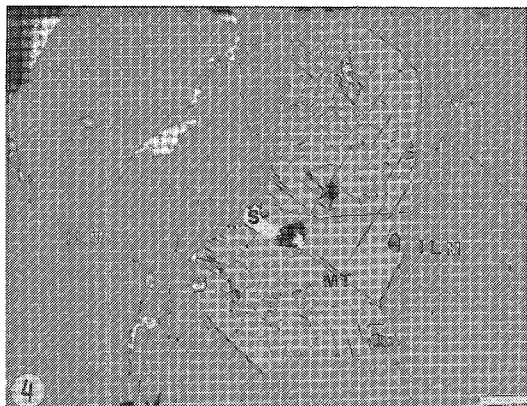
FIG. 4. Medium grey host is ilmenite, ILM. Light grey, large inclusion is titanomagnetite (MT) with lamellae of exsolved spinel (black) and oxidized–exsolved lamellae of ilmenite (difficult to see). Within titanomagnetite is white inclusion of chalcopyrite and pyrrhotite (s). Reflected light, oil immersion. Scale bar 50 μm. Inco sample DG–8.
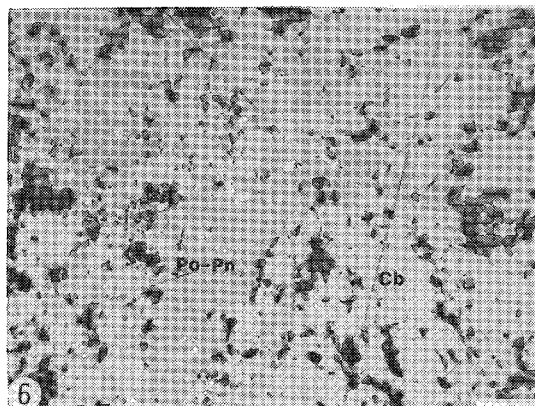

FIG. 6. Pyrrhotite (medium grey) with pentlandite inclusions (small, bright white), replaced by massive cubanite (light grey). No chalcopyrite observed. In some areas, pentlandite forms inclusions in cubanite. Reflected light, oil immersion. Scale bar 50 μm. Inco sample DG–7.

sulfides. These are found in both the Inco and AMAX samples. Polyphase sulfide bodies commonly mantle and appear to replace biotite and Fe–Ti oxides. Cu–Fe sulfides, in some cases, fill cleavage interfaces in biotite grains. Only rarely are sulfide bodies enclosed in Fe–Ti oxides. However, in almost every case in which the enclosing oxide is a coarse intergrowth of ilmenite and oxidized – exsolved titanomagnetite, the sulfide body is next to the magnetite (Fig. 4). There are many examples of sulfides replacing magnetite in magnetite–ilmenite intergrowths (Fig. 5).

Many examples in the Inco and Minnamax specimens also confirm Boucher's (1975) and Bonnichsen's (1972) interpretations that Cu–Fe sulfides commonly replaced earlier pyrrhotite. Irregular islands of pyrrhotite occur in cubanite or chalcopyrite
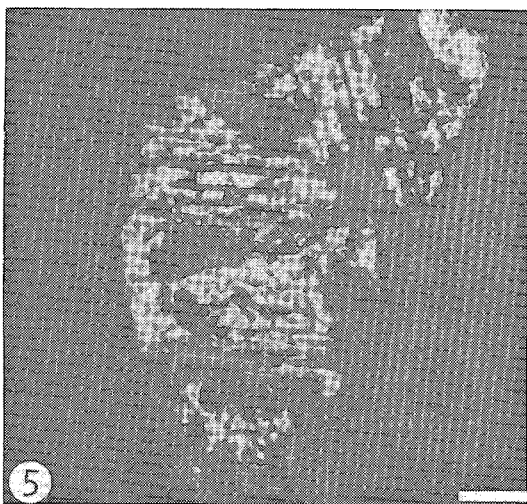

FIG. 5. Remnant of lamellar intergrowth of magnetite and ilmenite (i.e., oxidized–exsolved titanomagnetite). Cu–Fe sulfide (white) has selectively replaced magnetite and left ilmenite (dark grey lamellae). Reflected light, oil immersion. Scale bar 8 μm. Inco sample DG–2.
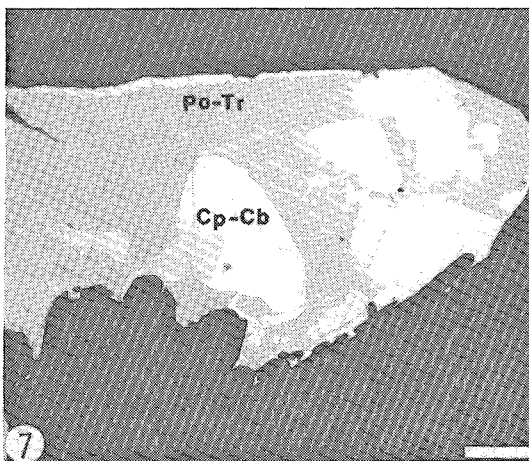

FIG. 7. Major phase (medium grey) is troilite, with lighter lamellae of pyrrhotite (48 at.% Fe). Round inclusions are lamellar intergrowths of chalcopyrite (white) and cubanite (light grey). Appears to have been coexisting pyrrhotite solid-solution and blebs of Cu–Fe-sulfide liquid (iss). Reflected light, oil immersion. Scale bar 50 μm. Minnamax drill-core 146, 558 m depth.
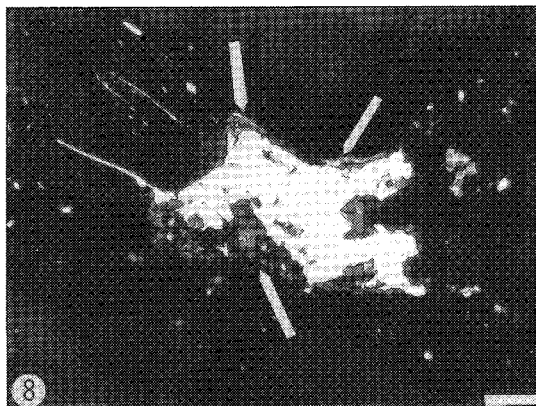
FIG. 8. Irregular bleb of pyrrhotite surrounded by rim of very finely crystalline graphite (arrows). Enclosed in serpentine vein. Reflected light, oil immersion. Scale bar 20 μm. Minnamax drill-hole 146, 173 m depth.

(or both), and residual pentlandite bodies are isolated in the two phases (Fig. 6). Chalcopyrite and cubanite can both be seen enclosing pentlandite grains and filling abundant fractures in the pentlandite (cf. Boucher 1975). In one sample, however, chalcopyrite fills fractures in a pentlandite grain that is fully enclosed in cubanite, indicating that cubanite locally may postdate and replace chalcopyrite.

Sulfide–sulfide textures differ among the individual samples, but there are no obvious distinc-
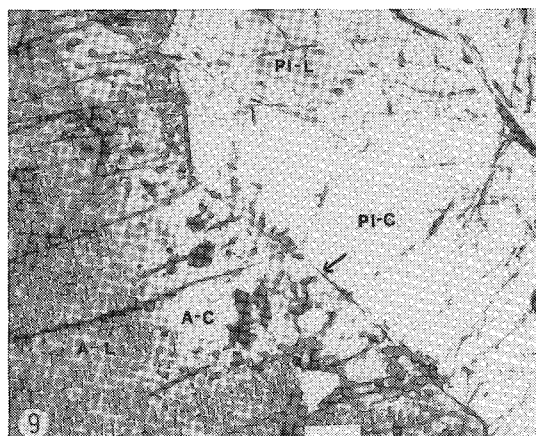

FIG. 9. Adjacent grains of augite (A) and plagioclase (Pl); arrow shows mutual grain-boundary. In each case, it appears that a cumulus core contains oxide (mostly magnetite) lamellae (–L), whereas adcumulus overgrowths (–C) do not. See Table 4 for plagioclase compositions. Transmitted light. Scale bar 500 μm. Inco sample DG-8.

tions between the Inco and Minnamax suites. There are some mineralogical distinctions, however, as indicated in Table 1 and discussed in a later section. Almost all the samples from both localities contain cubanite and chalcopyrite (or phases of similar composition). In some cases, the chalcopyrite (Cp) and cubanite (Cb) occur as lamellar intergrowths with each other. In a few samples, lamellar Cp–Cb occurs in round bodies enclosed in coarse grains of pyrrhotite (Fig. 7). The lamellar intergrowth probably resulted from the subsolidus exsolution of a higher-temperature Cp_{ss} phase. In some cases, however, chalcopyrite and cubanite form distinctly separate regions in a sulfide body, or cubanite occurs almost to the exclusion of chalcopyrite in a sample. The former case may represent textural reequilibration of exsolved bodies, but the latter case requires another explanation (see discussion section). In those samples in which there is a strong association of sulfides with plagioclase, massive cubanite appears dominant over chalcopyrite. In contrast, pyrrhotite seems to be the dominant phase in sulfide segregations associated with biotite.

Bornite is one of the minor sulfide phases. It occurs only in disseminated, fine-grained sulfide bodies, not in the larger interstitial segregations. Bornite usually comprises the lesser component of Cp–Bn and, more rarely, of Cp–Pn–Bn intergrowths (see Table 2).

Other opaque phases

In the Inco and Minnamax samples, titanomagnetite, ilmenite and graphite occur. Graphite occurs in two forms, which together usually comprise much less than 1% of individual samples. There are isolated blades (>100 μm) and clusters of blades between and within silicate grains (Hollister 1980), which may be xenolithic fragments from the wall rock. In addition, extremely fine-grained graphite (on the order of a few micrometres) occurs along some silicate grain-boundaries, in fine fractures in silicates, and as thin rims around sulfide segregations (Fig. 8). The latter may be a magmatic precipitate.

Ilmenite and titanomagnetite characteristically occur (Fig. 4) as large (up to several millimetres), anhedral intercumulus bodies, as smaller round inclusions in plagioclase and mafic phases, and as oriented rods (~3 × 12 μm) in plagioclase and clinopyroxene (Fig. 9). The coarser oxide grains commonly are associated with intercumulus pyroxene and biotite and, in many cases, with sulfides. Ilmenite grains are unzoned and have no exsolution bodies (confirmed by EDS analysis). The magnetite averages about 4-8 wt.% TiO_2 and commonly has abundant exsolution lamellae of spinel (*sensu stricto*), ulvöspinel and ilmenite (Fig. 4). In the Inco samples,

TABLE 3. REPRESENTATIVE BULK COMPOSITIONS OF PENTLANDITE

Sample*	A (7)		B (2)		C (3)		D (2)		E (6)		F (4)		G (1)
				Compositions in weight percent									
Fe	23.32	(.28)	26.64	(.65)	30.80	(.35)	32.29	(.18)	31.36	(.38)	33.15	(.54)	35.89
Ni	42.72	(.41)	37.60	(.18)	35.12	(.41)	33.20	(.13)	34.61	(.40)	32.78	(.54)	29.88
Cu	0.57	(.14)	0.64	(.50)	0.02	(.04)	0.04	(.05)	0.12	(.17)	0.0	(0)	0.25
Co	0.97	(.04)	1.21	(.01)	0.99	(.12)	1.63	(.01)	1.31	(.03)	1.32	(.12)	1.10
S	32.78	(.18)	33.24	(.09)	33.55	(.29)	33.48	(.13)	33.37	(.44)	32.51	(.34)	33.37
Total	100.36	(.84)	99.33	(.13)	100.48	(.46)	100.64	(.25)	100.77	(.77)	99.76	(.32)	100.49
			Compositions in atomic percent (normalized to Fe+Ni+S = 100)										
Fe	19		22		25		26		26		27		30
Ni	33		30		27		26		27		26		23
S	48		48		48		48		47		47		47

*Parentheses after sample number indicate number of analyses that were averaged.
Parentheses after wt.% analyses show one standard deviation.

A: 146-1176 (AMAX) small Pn-Cp compound grain. B: 146-469 (AMAX) Cp-Bn-Pn compound grain. C: 146-569 (AMAX) Pn matrix of Pn with fine lamellae. D: DG4 (INCO) large Pn inclusion in Po. E: 146-1443 (AMAX) large, isolated Pn. F: DG4 (AMAX) large Pn in large Cp hosted by Po. G: DG7 (INCO) Pn-Tr small compound grain. Electron-microprobe data.

coarse ilmenite and coarse magnetite grains commonly are directly adjacent (Pasteris 1983, in prep.).

COMPOSITION OF SULFIDE MINERALS

Approximately 200 electron-microprobe analyses (Tables 2, 3) were performed on 8 doubly polished thin sections (3 from Inco, 5 from Minnamax). The compositions of cubanite and chalcopyrite are nearly stoichiometric and do not vary systematically between the samples. The only "pyrrhotite" phases present are Fe_9S_{10} (hexagonal) and troilite, with hexagonal pyrrhotite occurring in both suites. As recognized optically, abundant coarse troilite occurs only in the Minnamax samples, usually with lamellar intergrowths of hexagonal pyrrhotite. Some small intercumulus compound grains of troilite and other sulfides were identified by WDS in the Inco suite.

Another phase with little compositional variation among the samples is Ni-mackinawite (Table 2). It appears to be a secondary phase, as is typical for mackinawite. This sulfide occurs as narrow stringers in serpentinized olivine, as large feather-like inclusions in chalcopyrite and cubanite, and as isolated rough-textured blebs that may be associated with pentlandite or cubanite. The phase is slightly metal-rich compared to troilite and contains approximately 5 wt.% Ni.

The compositionally most variable phase is pentlandite (Table 3). Even within a single thin section, the Fe content of the pentlandite varies up to 9 wt.%. However, no significant zoning was found within individual grains. Figure 10 is a plot of representative compositional groups of pentlandite (approximately 70 individual compositions) and their coexisting Fe sulfides. Generalizations are difficult to make. However, the following broad compositional patterns were observed among the mineralogical associations: 1) low-Ni pentlandite in

Pn-Tr, 2) moderate-Ni pentlandite for Pn-Po-Cp associations, stringers in silicate, coarse Pn in Po, isolated Pn in silicates, Pn remnants in Cb, 3) moderate- to high-Ni pentlandite in Cp-Bn-Pn and Pn-Cp associations, and 4) high-Ni pentlandite where extremely fine lamellae of Cp cross-cut the pentlandite. It therefore appears that the most Ni-rich pentlandite occurs in the most Cu-rich assemblages. In comparison, Weiblen & Morey (1976) reported 26-28 atomic % Ni in all of their samples of pentlandite, placing them in the moderate-Ni group.

Thin sections 146-569 and 146-1176 from Minnamax have the most Ni-rich compositions of pentlandite studied, although the same sections also contain typical, moderate-Ni grains. Sample 146-1176 also has the most oxidized Fe-Ti oxide assemblage that was analyzed from the Minnamax suite (Pasteris 1983, in prep.). In at least two cases, the high-Ni pentlandite contains very fine lamellae of chalcopyrite (Fig. 11). In one example, the pentlandite also is hosted by chalcopyrite, but in the other case, the pentlandite is isolated between silicate grains.

Minor minerals: presence and absence

Several minerals of low abundance were identified by electron-microprobe analysis. Small subhedral grains (not the typical "exsolution stars") of Fe-rich sphalerite (approximately 12 wt.% Fe) were found in a large chalcopyrite grain in Inco sample DG4 (see also Boucher 1975). In AMAX sample 146-1787, a 150-μm round inclusion of approximate composition $(Ni,Cu,Co)_3As_2$ was distinguished in coarse cubanite by EDS analysis (Fig. 12d). The grain contains approximately 50 wt.% Ni, 4 % Cu, and 3 % Co, As apparently being the only other component. The arsenide is whiter and has a higher reflec-
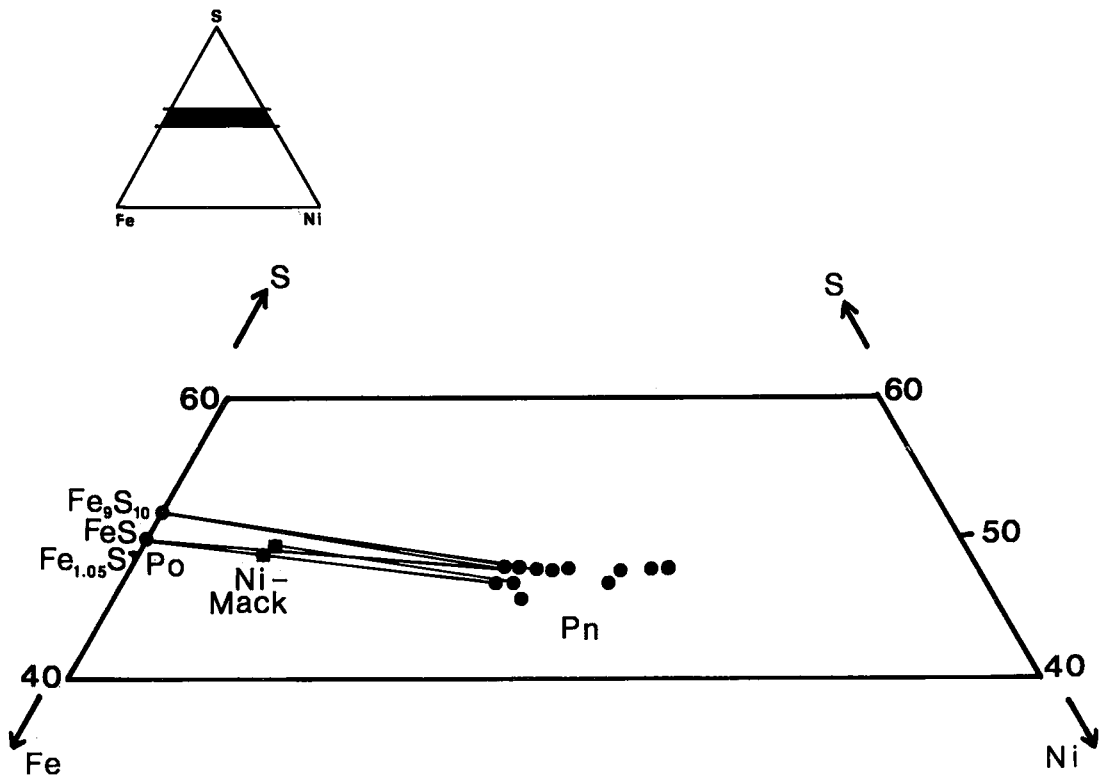
FIG. 10. Representative compositions of sulfides, normalized to Fe + Ni + S = 100 at.%, showing coexisting pentland-
ite and Fe sulfides. See Table 2 for descriptions of pyrrhotite and Ni–mackinawite samples, Table 3 for pentlandite
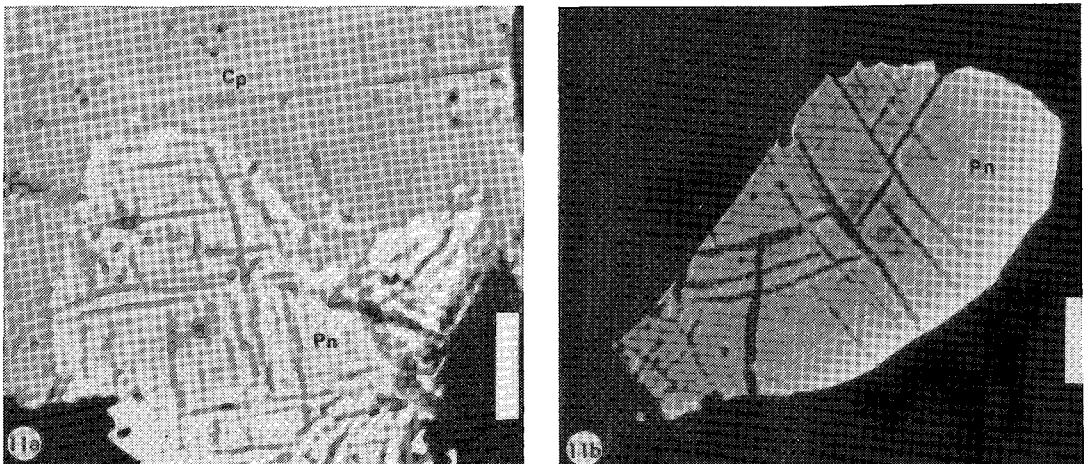descriptions.

FIG. 11. Back-scattered electron images of very fine lamellae (dark grey) of chalcopyrite in pentlandite. a. Chalcopyrite-
pentlandite intergrowth on edge of small grain of chalcopyrite. Minnamax sample 146–1176. b. Pentlandite grain
isolated in plagioclase. Minnamax sample 146–569. See Table 3 and Figure 10 for pentlandite compositions. Images
photographed at 15 kV exciting voltage; scale bar 10 μm.

tance than pentlandite. In comparison to its cubanite host, the arsenide appears almost metallic white and has approximately the same hardness as cubanite. In crossed polarizers, the phase shows a fine-grained mosaic structure and is weakly anisotropic (cf. oregonite, as in Antun et al. 1966). The one identified grain of heazlewoodite contains minor Fe and Cu, but no Co (Table 2).

The presence of Ni-mackinawite (see also Weiblen & Morey 1976) was discussed above. Owing to the wide range of optical properties, in spite of the limited range of compositions determined, this "phase" probably represents several stages of low-temperature breakdown products in addition to true mackinawite (cf. Antun et al. 1966). An occasional companion of mackinawite in Cu–Ni–Fe sulfide occurrences, the sheet silicate – sulfide valleriite (see Antun et al. 1966) was not identified. However, several 10–15-μm-wide lamellae with the optical features of mackinawite or valleriite were observed in coarse, octahedrally fractured pentlandite in a large grain of pyrrhotite. EDS analysis showed these veinlets probably to contain Mg-serpentine.

Following the work of Hardyman (1969) and Weiblen & Morey (1976), sulfides of the so-called chalcopyrite group (talnakhite, mooihoekite, haycockite) were sought among the disseminated

sulfides resembling tarnished chalcopyrite. The above phases were not detected, nor was Hall's & Weiblen's (1967) phase X (Fe-rich chalcopyrite). However, several grains of a metal-poor, Cu-rich "chalcopyrite" (Cp? in Table 2) and a metal-poor, Cu-poor bornite (Bn? in Table 2), locally intergrown, were documented in AMAX samples 146–569 and 146–1176. These two samples are also distinguished by the abundance of bornite and the presence of Ni-rich pentlandite filled with minute lamellae of chalcopyrite. The samples may be exihibiting partial exsolution (Cp–Bn, Pn–Cp) during re-equilibration.

Three other mineralogical features were noted that differ from the results and interpretations of Weiblen & Morey (1976) for their samples from the South Kawishiwi intrusive complex ("Inco"). In the present study, only troilite and hexagonal pyrrhotite were identified by electron-microprobe analysis (in agreement with Boucher 1975), not hexagonal and monoclinic pyrrhotite. Weiblen & Morey (1976) reported that they found no monomineralic pentlandite assemblages, whereas they do appear in the present suite as both small and coarse grains. In addition, the cubanite grains in the present study are consistently nonstoichiometric. Values of the metal:sulfur ratio are 3:3 (Table 2), but the grains
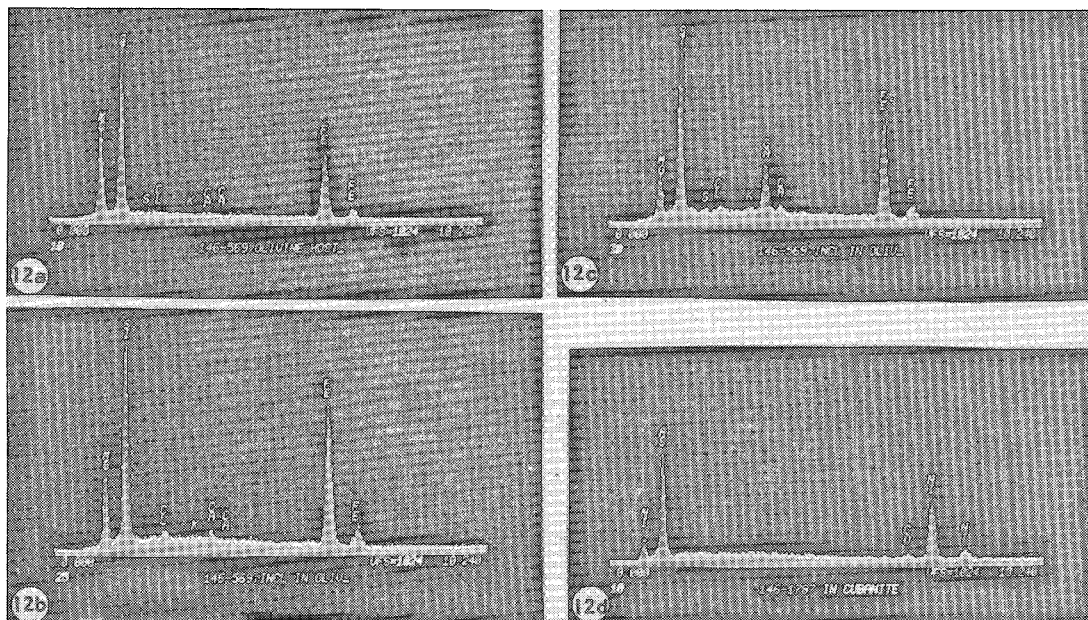

FIG. 12. Energy-dispersion spectra at 15 kV; counting time (in seconds) recorded at far left base of spectrum; full vertical scale 1024 counts. Sample number listed under each spectrum. a. Olivine grain host to multiple pits that are probably opened fluid inclusions. b, c. Analyses of the pits show Ca and Cl in both cases, as well as K and S in one case. The pits may be remnants of brine-filled fluid inclusions. d. Analysis of a 200-μm elliptical inclusion in a large grain of cubanite. It is a Ni arsenide with a few wt.% Co and minor Cu.

are commonly Fe-rich. This may reflect the incomplete reaction of Cu–Fe sulfide species with pre-existing Fe sulfides.

SIGNIFICANCE OF SULFIDE TEXTURES
AND MINERALOGY

As recognized by Bonnichsen (1972), Boucher (1975) and Weiblen & Morey (1976), almost all of the sulfide separation in the troctolites occurred considerably below the liquidus, presumably as an immiscible melt. The sulfides are interstitial and vein-like; those that occur as inclusions in plagioclase are in adcumulus overgrowths or in intercumulus grains. The textures do not support a cause-and-effect relationship between the precipitation of sulfides and of Fe–Ti oxides. Thus, there is little evidence that sulfide segregation was induced by a sudden decrease in iron content of the melt as oxides began to precipitate. Primary magnetite is rarely found in the sulfide bodies, suggesting that the immiscible sulfide melt did not have an oxygen content as high as that reported in other igneous environments (cf. Skinner & Peck 1969).

Several inferences follow from the specific compositions of sulfides and assemblages found in the two troctolites. A low-sulfur bulk composition for the parent melts is indicated by 1) the lack of monoclinic pyrrhotite (a common FeS phase in many other deposits) in preference to hexagonal pyrrhotite ± troilite in both suites, 2) the lack of sulfur-rich phases such as pyrite, and 3) the presence of the metal-rich phase heazlewoodite (in one section from 146–569; see Table 2). The apparent inconsistency between low fugacity of sulfur and abundant sulfide minerals is explained by the self-buffering capacity of sulfide-rich rocks (cf. Eckstrand 1975).

The compositions and assemblages of the sulfides also show a lack of equilibration and suggest more than one episode of sulfide precipitation or re-equilibration. For instance, the observed assemblages Cp–Tr and Cp–hPo are metastable with respect to Cb–Tr and Cb–hPo (Craig & Scott 1974). This may account for the reaction relationship observed in both troctolite suites between Fe sulfides and Cu–Fe sulfides.

Previous studies of the system Fe–Ni–S have shown that in natural and artificially produced assemblages, the composition of the pentlandite grains is closely correlated with the specific mineralogy of the coexisting sulfides (e.g., Graterol & Naldrett 1971, Harris & Nickel 1972, Misra & Fleet 1973, Craig 1973). In the two suites under investigation, there is no consistent compositional distinction between pentlandite coexisting with hexagonal pyrrhotite alone and that coexisting with troilite (Fig. 10). Most samples of pentlandite are in the range 25–27 at.% Ni and 25–27 at.% Fe. Some grains are

somewhat richer in Fe; others are very enriched in Ni (Fig. 10). The cobalt content of all the pentlandite samples is about 1–2 wt.%. The most Fe-rich grains, which coexist with Fe sulfides, texturally appear to be primary. Their compositions (23–24 at.% Ni) plot between the compositional ranges reported by Misra & Fleet (1973) for the natural assemblages Tr–Pn (lower Ni) and Tr–hPo–Pn (higher Ni).

The composition of the high-Ni pentlandite from compound grains of Cp–(Bn)–Pn and the high-Ni pentlandite (30–33 at.% Ni) with fine Cp lamellae corresponds to that usually found in more sulfur-rich assemblages, such as those containing pyrite, and more Ni-rich assemblages, such as those with millerite, heazlewoodite and godlevskite (Misra & Fleet 1973). No pyrite was identified at Duluth, and only one grain of Fe-bearing heazlewoodite (Table 2) was found near a Ni-rich Pn.

These textural and compositional data on the sulfides suggest that at least two episodes of sulfide mineralization occurred, and that the products now observed represent (partial) re-equilibration below 200°C. The early mineralization was dominated by a homogeneous, low-sulfur Fe–(Ni–)S phase (mss) and intermediate solid-solution (iss of the Cu–Fe–S system). Subsequent re-equilibration eventually produced the coexisting intergrowths of Tr–hPo and Cp–Cb (Fig. 7). According to accepted interpretations of the phase assemblages (e.g., Craig 1973), pentlandite should have formed from the Fe–(Ni–)S phase at about 600°C. However, large coarse grains of Pn with or without Po and small, intercumulus Pn grains (isolated, with chalcopyrite alone or, rarely, with Po) are abundant. This raises the questions: 1) could Pn be a liquidus phase? (unlikely); 2) was there extensive, late-stage silicate–sulfide recrystallization at Duluth? (probably); and 3) did some pre-existing compositions of pentlandite become enriched in Ni during subsequent re-equilibration? (possibly). The Ni-rich phase heazlewoodite (stable below ~556°C) typically is regarded as a product of the reduction of pentlandite during serpentinization (Craig & Scott 1974). However, the Fe (~2 wt.%) and Cu (~1.3 wt.%) contents of the one analyzed grain of heazlewoodite suggest a possible higher-temperature, primary origin.

An episode of later mineralization or, at least, later re-equilibration affected large portions of the sulfides. This is most clearly observed in the widespread replacement of Fe sulfides by cubanite and chalcopyrite. Replacement could explain the common occurrence of small grains of pentlandite in massive cubanite (Fig. 6) and the abundance of massive cubanite in the absence of chalcopyrite. The high content of Ni in some small, intercumulus Pn grains coexisting with chalcopyrite (some of the most Ni-rich Pn compositions shown in Fig. 10) could be

TABLE 4. REPRESENTATIVE BULK COMPOSITIONS OF SILICATE MINERALS

Sample*	A	B	C	D	E	F	G	H	I	J	K	L
SiO_2 wt.%	53.16	47.75	53.90	52.83	50.36	35.92	36.05	36.69	36.98	37.12	35.61	36.49
K_2O	0.30	0.07	0.32	0.29	0.15	0.0	0.0	0.0	0.0	0.0	0.0	0.0
TiO_2	0.02	0.03	0.11	0.13	0.02	0.0	0.0	0.0	0.19	0.07	0.0	0.0
Al_2O_3	27.94	31.57	27.53	27.92	29.81	0.0	0.0	0.0	0.0	0.0	0.0	0.0
MgO	0.02	0.0	0.03	0.02	0.01	28.57	27.83	32.43	32.11	32.99	29.43	30.27
CaO	13.02	17.25	12.69	13.02	15.53	0.05	0.05	0.01	0.01	0.03	0.02	0.03
Na_2O	3.82	1.73	4.27	3.97	2.84	0.0	0.0	0.0	0.0	0.0	0.0	0.0
MnO	--	--	--	--	--	0.52	0.57	0.39	0.44	0.42	0.53	0.51
FeO	0.18	0.80	0.21	0.27	0.27	35.81	36.68	30.62	31.39	30.21	34.30	33.93
NiO	--	--	--	--	--	0.14	0.11	0.18	0.20	0.21	0.21	0.23
Cr_2O_3	0.0	0.0	0.0	0.0	0.0	0.0	0.02	0.01	0.03	0.06	0.0	0.0
Total	98.46	99.17	99.06	98.45	98.99	101.01	101.31	100.33	101.35	101.11	100.10	101.46
An (Fo)	64	84	61	63	75	59	58	65	65	66	60	61
Ab (Fa)	34	15	37	35	25	41	42	35	35	34	40	39
Or	2	1	2	2	0							

* indicates that the element was not analyzed for. A, B: DG3 (INCO), core (A) and clear edge (B) of plagioclase grain. C, D, E: DG3, core (C), core near oxide lamellae (D) and edge (E) of plagioclase. F: 146-569 (AMAX) large grain of olivine. G: 146-569 small grain of olivine. H: DG3 large, subhedral grain of olivine. I: DG4 (INCO) olivine with trail of fluid inclusions. J: DG4 olivine with fine Fe-Ti oxide lamellae. K: DG7 (INCO) large grain of olivine. L: DG7 small grain of olivine. Each column represents the results of one electron-microprobe analysis.

due to partial re-equilibration at this time. These distinctive compositions also might be due to the late-stage influx of more Ni- and Cu-rich sulfides. The presence of massive cubanite and troilite constrains the temperature of final reaction to below about 200°C and about 140°C, respectively.

Other mineralogical evidence suggests that this later episode was a distinct event of mineralization involving copper enrichment. The disseminated sulfides in adcumulus plagioclase grains are Cu-rich compared to the commonly more massive interstitial sulfides (Boucher 1975, Weiblen & Morey 1976; this study). Cu–Fe sulfides selectively replace exsolved Fe–Ti oxides (Fig. 5) that have equilibration temperatures from about 700°C to 900°C (Pasteris 1983).

The apparent Cu-enrichment trend, in part, may reflect the normal fractionation of a mafic melt as it acquires an increasing Cu:Ni ratio. Experiments in the system Cu–Fe–Ni–S (e.g., Craig & Kullerud 1969) indicate that as temperature decreases, the sulfide liquid coexisting with solid pyrrhotite will become increasingly Cu-rich. Thus, simple fractionation may account for the confinement of the high-(Cu:Fe) phase bornite to late-stage sulfide disseminations.

However, it is clear that the silicates (and presumably also the sulfides) at Duluth have undergone more than simple fractionation (Foose 1982, Tyson & Chang 1984). Weiblen & Morey (1976) reported that the plagioclase rims that enclose Cu-rich sulfides are more anorthite-rich than the cores of the grains; similarly, in ferromagnesian grains with marginal sulfide inclusions, the silicate rims are more Mg-rich than the cores. Further analysis was done in the present study to evaluate the pervasiveness and significance of this effect.

Electron-microprobe analysis shows a consistent increase in Ca with accompanying decrease in Na and, to a lesser extent, K from the core of plagioclase grains to their sulfide-enclosing rim. The core–rim differences reach 4 wt.% CaO (Table 4).

The same compositional populations of plagioclase are defined by the cores of grains filled with lamellae (spinel, magnetite, ilmenite) and their clear, often irregular, nonlamellar rims (Fig. 8). Cathodoluminescence microscopy showed the same scale of compositional distinctions between apparent early cumulates (with oxide lamellae) and later adcumulates (without lamellae).

The silicates, therefore, appear to have undergone some hiatus during their growth. In particular, they were undergoing adcumulus growth or dissolution and reprecipitation during late-stage sulfide mineralization. At this time, the Fe and Ti contents of the melt had decreased sufficiently to prevent the previously widespread development of oxide lamellae in the grains of plagioclase and augite (Fig. 8).

CONTROLS ON THE TIMING AND LOCALIZATION OF SULFIDE PRECIPITATION

There is ongoing discussion about how sulfide segregation was initiated at Duluth, from where were the sulfur and metals derived, and how can the particular localization of and compositional variations in the sulfide mineralization be explained (e.g., Bonnichsen 1972, Boucher 1975, Weiblen & Morey 1976, Mainwaring & Naldrett 1977, Ripley 1981). The sulfur-isotope work of Mainwaring & Naldrett (1977) and Ripley (1981) gives strong backing to Mainwaring's & Naldrett's (1974) original suggestion that much of the sulfur was derived from the sediments intruded by the Duluth Complex. An inherent part

of such a process is the large-scale transport and mixing of the sulfur in the melt.

The development and evolution of a high-temperature fluid phase seem critical to the explanation of the Duluth sulfides. Ripley (1981) has discussed some of the thermodynamics of producing fluids that contain H_2O, H_2S, CO_2 and CH_4. Physical evidence for the passage of fluids over a range in temperature is found in the abundance of fluid inclusions (mostly empty now) along healed fractures in the silicates and apatite, by the presence of stringers of microcrystalline graphite in the silicates, and by the occurrence of irregular veinlets of low-temperature Ni-bearing mackinawite in serpentinized olivine (Fig. 3). The texture of the fine-grained, fracture-filling graphite suggests that it was vapor-deposited (cf. Frost 1979). More information on the temperature and $f(O_2)$ of the fluid is required to determine from what vapor species the carbon precipitated (cf. Pasteris 1981). The narrow, irregular veinlets of iron sulfides in altered olivine probably were produced when iron from the original olivine was excluded during serpentinization, in the presence of mobile, sulfur-bearing fluids (cf. Eckstrand 1975, Groves & Keays 1979).

The close association of presumably magmatic carbon and sulfides has been noted in other igneous suites (e.g., Pasteris 1981, Pedersen 1981, Elliott et al. 1982). It may reflect $f(O_2)$ control on the timing of sulfide segregation because the presence of graphite in the assemblage constrains the $f(O_2)$ (e.g., Ohmoto & Kerrick 1977, Frost 1979, Ripley 1981). Buchanan & Nolan (1979) experimentally produced immiscible sulfide liquids in sulfide-saturated melts at different fugacities of oxygen. They demonstrated that a much higher value of $f(S_2)$ is necessary to nucleate an immiscible sulfide phase in a high-$f(O_2)$ than in a low-$f(O_2)$ melt (for instance, over the log $f(O_2)$ range -8.50 to -11.50 at $1200°C$). However, they also demonstrated that for a given temperature and $f(S_2)$ in a sulfur-undersaturated liquid, the reduced melt could dissolve much more sulfur than the oxidized melt before a sulfide liquid was segregated (cf. Haughton et al. 1974). In addition, this reduced melt would be very sensitive to slight increases in $f(S_2)$ and $f(O_2)$, which could lead to the nucleation of an immiscible liquid.

The particular T-$f(O_2)$ conditions in the Duluth magmas (as controlled by graphite and coexisting phases) are considered to have caused sulfide saturation to be delayed until late in the magmatic sequence. Sulfide saturation postdated the precipitation of most of the olivine, and coincided with the precipitation of biotite and other intercumulus phases. The Ni content of the olivine grains (~ 0.18–0.22 wt.% NiO for Fo$_{60-65}$) is only slightly higher than expected for coexisting sulfide and silicate melts (cf. Fleet & MacRae 1983). Both sulfur

(e.g.., Ferry 1981) and carbon species (e.g., Frost 1979) probably were mobilized from the wall rocks as volatile components and dissolved in the melt (e.g., Burnham 1979, Ripley 1981) without large-scale physical assimilation of xenoliths (cf. Grant & Molling 1981).

The pervasive influence of these volatiles on the $f(O_2)$ and $f(S_2)$ of the local igneous environment apparently is reflected in the mineralogy of individual deposits. In the samples from the Inco deposit, troilite is rare, but both coarse magnetite and ilmenite coexist, and the magnetite demonstrates subsolidus oxidation-exsolution. In contrast, samples from the Minnamax drill-core contain abundant troilite [requiring a lower sulfur:metal ratio than the other pyrrhotite phases, thus a lower $f(O_2)$], coarse ilmenite (but no magnetite), and veinlets of vapor-deposited graphite in association with the sulfides. A temperature-$f(O_2)$ analysis of the Fe-Ti oxides in both troctolites (Pasteris 1983, in prep.) shows the ilmenite–magnetite assemblages to approximate the quartz – fayalite – magnetite buffer, and the Minnamax ilmenite to lie at somewhat lower fugacities of oxygen.

CONCLUSIONS

The process of intercumulus infiltration in layered intrusive complexes, as described by Irvine (1980), may provide the key to understanding the evolution of the Duluth Complex. In part, the model allows for intercumulus liquid from an earlier, more primitive melt, from the base of a fractionating sequence, to percolate upward through the cumulates of a later, more fractionated sequence in a layered complex. It provides a means by which the following effects can be brought about: 1) the mineralogy and composition in the upper portion of an igneous sequence can be affected by the chemical parameters established early in the crystallization history (at the base of a sequence), 2) mineral compositions in the sequence can be given a more primitive signature than otherwise would occur, and 3) a more gradual evolution (as distinguished from episodic change) occurs in the intercumulus liquid as it partly re-equilibrates with successive batches of less primitive solids and intercumulus liquid. This mechanism is especially significant for the Duluth troctolites, which have a multi-injection history and in which the sulfides clearly are intercumulus products. The development of a high-temperature fluid is suggested to have been part of the overall intercumulus process at Duluth; in part, the fluid may account for the metasomatizing potential of the infiltrating intercumulus liquid.

In summary, sulfide mineralization in the Duluth troctolites may well reflect a two-stage process. Initially, volatiles (e.g., CO_2, H_2O, H_2S, CH_4) were

dissolved in the silicate melt at the time when an early immiscible sulfide liquid segregated. The sulfide had a high Fe:Cu ratio and subsequently crystallized primarily massive, interstitial pyrrhotite (with some exsolution products upon cooling). Later in the crystallization sequence, the volatiles separated from the silicate melt as a distinct phase, and contained considerable dissolved copper and sulfur. This fluid was capable of compositionally altering pre-existing phases. Thus, the three dominant textures of chalcopyrite and cubanite may represent a continuum from sulfide liquid immiscibility to high-temperature reaction of a fluid and a sulfide phase: 1) rounded bodies of lamellar Cp–Cb in Po (original coexistence of *iss* and Po$_{ss}$), 2) irregular, small islands of pyrrhotite ± pentlandite in a cubanite ± chalcopyrite host (partial replacement), and 3) homogeneous large bodies of cubanite (completed reaction FeS + CuFeS$_2$ → CuFe$_2$S$_3$). An active, late-stage Cu- and S-bearing fluid would account for the selective replacement by Cu–Fe sulfide of magnetite regions in oxidized and exsolved magnetite–ilmenite intergrowths (Fig. 5), for cubanite bodies that appear pseudormorphic after biotite and titanomagnetite, and for Cu–Fe sulfides replacing interstitial pyrrhotite in troctolite and xenolith assemblages (Fig. 2).

This fluid phase is considered to have evolved with, but to have been more mobile than, the intercumulus liquid. As distinct from the typical model of a hydrothermal fluid, this magmatic fluid contained relatively little water and was of higher temperature. In the present study, preliminary fluid-inclusion analysis by laser Raman spectroscopy (*cf.* Rosasco & Roedder 1979) revealed small amounts of CO$_2$ in some fluid inclusions. Microthermometry was unsuccessful in detecting phase changes upon cooling down to –196°C; the inclusions may now be empty. However, the energy-dispersion electron-microprobe analysis of some opened, 10–20 μm pits in olivine grains in polished thin section (Figs. 12a–c) reveals the presence of Ca (abundant, commonly detected), S (low abundance, rare) and Cl (low abundance, rare). The end stages of the fluid phase may have been a CO$_2$-bearing brine with dissolved metals such as Cu [see Candela & Holland (1982) on Cu partitioning]. A low content of water would account for the reported lack of pervasive alteration of the affected rocks, but some of the finer-grained intercumulus silicate patches (with sulfides) actually show strong secondary alteration.

The evolution of the $f(O_2)$ and $f(S_2)$ of the fluid was punctuated by influxes of H$_2$O, CO$_2$ and H$_2$S from wallrock assimilation. Because the fluid is envisioned as compositionally evolving over time, however, sudden large influxes of volatile species are not required to produce sulfide immiscibility. Upper zones of Cu-rich disseminated sulfides, such as the "cloud zone" in the Minnamax deposit, reflect the effect of this evolving fluid on $f(O_2)$, $f(S_2)$ and sulfur content and capacity of the melt. At some point in its fractionation, cooling and assimilation, the melt again became sulfide-saturated. The irregularities in the sulfur-isotope data (Ripley 1981) may reflect the fact that some of the analyzed sulfides are direct precipitates of a sulfide liquid, whereas others have undergone reaction with a later, sulfide-bearing fluid.

The present study is based on a small number of samples, so that only broad-based interpretations are possible. However, it is significant that there are obvious distinctions in the opaque mineralogy between the two adjacent bodies of troctolite. This is important for future evaluation of these deposits for both their Cu–Ni and Ti contents. Future studies should address changes in the sulfide and oxide mineralogy with depth in several drill-cores.

REFERENCES

ALBEE A.L. & RAY, L. (1970): Correction factors for electron probe microanalysis of silicates, oxides, carbonates, phosphates and sulfates. *Anal. Chem.* **42**, 1408-1414.

ANTUN, P., EL GORESY, A. & RAMDOHR, P. (1966): Ein neuartiger Typ "hydrothermaler" Cu–Ni-Lagerstatten. *Mineral. Deposita* **2**, 113-132.

BENCE, A.E. & ALBEE, A.L. (1968): Empirical correction factors for the electron microanalysis of silicates and oxides. *J. Geol.* **76**, 382-403.

BONNICHSEN, B. (1972): Sulfide minerals in the Duluth Complex. *In* Geology of Minnesota: a Centennial Volume (P.K. Sims & G.B. Morey, eds.). *Minn. Geol. Surv. Spec. Vol.*, 388-393.

_____ (1974): Copper and nickel resources in the Duluth Complex, northeastern Minnesota. *Minn. Geol., Inf. Circ.* **10**.

BOUCHER, M.L. (1975): Copper–nickel mineralization in a drill core from the Duluth Complex of northern Minnesota. *U.S. Bur. Mines Rep. Invest.* **8084.**

BUCHANAN, D.L. & NOLAN, J. (1979) Solubility of sulfur and sulfide immiscibility in synthetic tholeiitic melts and their relevance to Bushveld-Complex rocks. *Can. Mineral.* **17**, 483-494.

BURNHAM, C.W. (1979): Magmas and hydrothermal fluids. *In* Geochemistry of Hydrothermal Ore Deposits (2nd edition; H.L. Barnes, ed.). Wiley-Interscience, New York.

CANDELA, P.A. & HOLLAND, (1982): The partitioning of copper and molybdenum between magmas and hydrothermal fluids. *Geol. Soc. Amer. Abstr. Program* **14**, 458.

COOPER, R.W., MOREY, G.B. & WEIBLEN, P.W. (1978): Topographic and aeromagnetic lineaments and their relationship to bedrock geology in a glaciated Precambrian terrane, northeastern Minnesota. *In* Proc. Third Int. Conf. Basement Tectonics (D.W. O'Leary & J.L. Earle, eds.). Basement Tectonics Committee Inc., Denver, Colorado.

CRAIG, J.R. (1973): Pyrite–pentlandite assemblages and other low temperature relations in the Fe–Ni–S systems. *Amer. J. Sci.* **273-A**, 496-510.

_____ & KULLERUD, G. (1969): Phase relations in the Cu–Fe–Ni–S system and their application to magmatic ore deposits *In* Magmatic Ore Deposits (H.D.B. Wilson, ed.). *Econ. Geol. Mon.* **4**, 344-358.

_____ & SCOTT, S.D. (1974): Sulfide phase equilibria. *In* Sulfide Mineralogy (P.H. Ribbe, ed.). *Mineral. Soc. Amer., Short Course Notes* **1**, CS1-110.

ECKSTRAND, O.R. (1975): The Dumont serpentinite: a model for control of nickeliferous opaque mineral assemblages by alteration reactions in ultramafic rocks. *Econ. Geol.* **70**, 183-201.

ELLIOTT, W.C., GRANDSTAFF, D.E., ULMER, G.C., BUNTIN, T. & GOLD, D.P. (1982): An intrinsic oxygen fugacity study of platinum–carbon associations in layered intrusions. *Econ. Geol.* **77**, 1493-1510.

FERRY, J.M. (1981): Petrology of graphitic sulfide-rich schists from south-central Maine: an example of desulfidation during prograde regional metamorphism. *Amer. Mineral.* **66**, 908-930.

FLEET, M.E. & MACRAE, N.D. (1983): Partition of Ni between olivine and sulfide and its application to Ni–Cu sulfide deposits. *Contr. Mineral. Petrology* **83**, 75-81.

FOOSE, M.P. (1982): Structural, stratigraphic, and geochemical features of the South Kawishiwi intrusion, Duluth Complex, Minnesota. *Geol. Soc. Amer. Abstr. Program* **14**, 490.

FROST, B.R. (1979): Mineral equilibria involving mixed volatiles in a C–O–H fluid phase: the stabilities of graphite and siderite: *Amer. J. Sci.* **279**, 1033-1059.

GRANT, N.K. & MOLLING, P.A. (1981): A strontium isotope and trace element profile through the Partridge River troctolite, Duluth Complex, Minnesota. *Contr. Mineral. Petrology* **77**, 296-305.

GRATEROL, M & NALDRETT, A.J. (1971): Mineralogy of the Marbridge no. 3 and no. 4 nickel–iron sulfide deposits, with some comments on low temperature equilibration in the Fe–Ni–S system. *Econ. Geol.* **66**, 879-900.

GROVES, D.I. & KEAYS, R.R. (1979): Mobilization of ore-forming elements during alteration of dunites, Mt. Keith – Betheno, Western Australia. *Can. Mineral.* **17**, 373-389.

HALL, H.T. & WEIBLEN, P.W. (1967): Ore minerals of the Duluth Gabbro Complex. *Geol. Soc. Amer. Spec. Pap.* **115**, 89-90.

HARDYMAN, R.F. (1969): *The Petrography of a Section of the Basal Duluth Complex, St. Louis County, Northeastern Minnesota.* M.S. thesis, Univ. Minnesota, Minneapolis, Minn.

HARRIS, D.C. & NICKEL, E.H. (1972): Pentlandite compositions and associations in some mineral deposits. *Can. Mineral.* **11**, 861-878.

HAUGHTON, D.R., ROEDER, P.L. & SKINNER, B.J. (1974): Solubility of sulfur in mafic magmas. *Econ. Geol.* **69**, 451-467.

HOLLISTER, V.F. (1980): Origin of graphite in the Duluth Complex. *Econ. Geol.* **75**, 764-766.

IRVINE, T.N. (1980): Magmatic infiltration metasomatism, double diffusive fractional crystallization, and adcumulus growth in the Muskox intrusion and other layered intrusions. *In* Physics of Magmatic Processes (R.B. Hargraves, ed.). Princeton University Press, Princeton, N.J.

MAINWARING, P.R. & NALDRETT, A.J. (1974): Genesis of Cu–Ni sulfides in the Duluth Complex. *Geol. Soc. Amer. Abstr. Program* **6**, 854-855.

_____ & _____ (1977): Country-rock assimilation and the genesis of Cu–Ni sulfides in the Water Hen intrusion, Duluth Complex, Minnesota. *Econ. Geol.* **72**, 1269-1284.

MISRA, K.C. & FLEET, M.E. (1973): The chemical composition of synthetic and natural pentlandite assemblages. *Econ. Geol.* **68**, 518-539.

OHMOTO, H. & KERRICK, D. (1977): Devolatilization equilibria in graphitic systems. *Amer. J. Sci.* **277**, 1013-1044.

PASTERIS, J.D. (1981): Occurrence of graphite in serpentinized olivines in kimberlite. *Geology* **9**, 356-359.

_____ (1983): Fe–Ti oxides in and the significance of fO_2 differences within the Duluth Complex. *Geol. Assoc. Can. – Mineral. Assoc. Can. Program Abstr.* **8**, A53.

PEDERSEN, A.K. (1981): Armalcolite-bearing Fe–Ti oxide assemblages in graphite-equilibrated salic volcanic rocks with native iron from Disko, central west Greenland. *Contr. Mineral. Petrology* **77**, 307-324.

RIPLEY, E.M. (1981): Sulfur isotopic studies of the Dunka Road Cu–Ni deposit, Duluth Complex, Minnesota. *Econ. Geol.* **76**, 610-620.

_____ & RAO, B.V. (1980): Oxygen isotopic studies of the Dunka Road Cu–Ni deposit, Duluth Complex, Minnesota. *Geol. Soc. Amer. Abstr. Program* **12**, 510.

ROSASCO, G.J. & ROEDDER, E. (1979): Application of a new Raman microprobe spectrometer to nondestructive analysis of sulfate and other ions in individual phases in fluid inclusions in minerals. *Geochim. Cosmochim. Acta* **43**, 1907-1915.

SKINNER, B.J. & PECK, D.L. (1969): An immiscible sulfide melt from Hawaii. *In* Magmatic Ore Deposits (H.D.B. Wilson, ed.). *Econ. Geol. Mon.* **4**, 310-322.

TYSON, R.M. & CHANG, L.L.Y. (1984): The petrology and sulfide mineralization of the Partridge River troctolite, Duluth Complex, Minnesota, *Can. Mineral.* **22**, 23-38.

WATOWICH, S.N. (1978): A preliminary geological view of the MINNAMAX copper– nickel deposit in the Duluth Gabbro. *Proc. 51st Ann. Meet., Minn. Sect. AIME, 39th Ann. Mining Symp.*, 19-1-19-11.

WEIBLEN, P.W. & MOREY, G.B. (1976): Textural and compositional characteristics of sulfide ores from the basal contact zone of the South Kawishiwi intrusion, Duluth Complex, northeastern Minesota. *Proc. 37th Ann. Mining Symp. (Minn. Geol. Surv. Reprint Ser.* **32**).